Arsenic immobilization via preconcentration of arsenic from dilute solution using schwertmannite followed by immobilization in Ca-Fe-AsO_4 compounds

Ilhwan Park [1,*], Takashino Ryota [2], Takeuchi Yuto [2], Carlito Baltazar Tabelin [3], Theerayut Phengsaart [4], Sanghee Jeon [1], Mayumi Ito [1] and Naoki Hiroyoshi [1]

[1] Division of Sustainable Resources Engineering, Faculty of Engineering, Hokkaido University, Sapporo 060-8628, Japan.

[2] Division of Sustainable Resources Engineering, Graduate School of Engineering, Hokkaido University, Sapporo 060-8628, Japan.

[3] School of Minerals and Energy Resources Engineering, University of New South Wales, Sydney 2052, NSW, Australia.

[4] Department of Mining and Petroleum Engineering, Faculty of Engineering, Chulalongkorn University, Bangkok 10330, Thailand.

* Correspondence: i-park@eng.hokudai.ac.jp

Abstract:

Acid mine drainage (AMD) with toxic arsenic (As) is commonly generated from the tailings storage facilities (TSFs) of sulfide mines due to the presence of As-bearing sulfide minerals (e.g., arsenopyrite, realgar, orpiment, etc.). To suppress As contamination to the nearby environments, As immobilization by Ca–Fe–AsO_4 compounds is considered one of the most promising techniques; however, this technique is only applicable when As concentration is high enough (> 1 g/L). To immobilize As from wastewater with low As concentration (~10 mg/L), this study investigated a two-step process consisting of concentration of dilute As solution by sorption/desorption using schwertmannite ($Fe_8O_8(OH)_{8-2x}(SO_4)_x$; where ($1 \leq x \leq 1.75$)) and formation of Ca–Fe–AsO_4 compounds. Arsenic sorption tests indicated that As(V) was well adsorbed onto schwertmannite at pH 3 (Q_{max} = 116.3 mg/g), but its sorption was limited at pH 13 (Q_{max} = 16.1 mg/g). A dilute As solution (~11.2 mg/L As) could be concentrated by sorption with large volume of dilute As solution at pH 3 followed by desorption with small volume of eluent of which pH is 13. The formation of Ca–Fe–AsO_4 compounds from As concentrate solution (2 g/L As(V)) was strongly affected by temperature and pH. At low temperature (25–50°C), amorphous ferric arsenate was formed, while at high temperature (95°C), yukonite ($Ca_2Fe_{3-5}(AsO_4)_3(OH)_{4-10}\cdot xH_2O$; where x=2–11) and

johnbaumite ($Ca_5(AsO_4)_3OH$) were formed at pH 8 and 12, respectively. Among the synthesized products, johnbaumite showed strongest As retention ability even under acidic (pH<2) and alkaline (pH>9) conditions.

Keywords: arsenic immobilization; adsorption/desorption; concentration; schwertmannite; ferric arsenate; yukonite, johnbaumite

1. Introduction

Mining, mineral processing, and pyro/hydrometallurgy are essential activities for the stable supply of metals. These activities, however, generate huge amounts of solid wastes—waste rocks/overburden, tailings, slags, fly ashes and leaching residues/sludge—that are hazardous to people and the surrounding environments (Park et al., 2019, 2020a; Tabelin et al., 2021). For example, waste rocks/overburden and tailings produced from mining and processing of sulfide ores contain non-valuable sulfide minerals like pyrite (FeS_2) and arsenopyrite (FeAsS), and when these kinds of sulfide-bearing wastes are exposed to water and oxygen, acid mine drainage (AMD) is generated due to their strong acidification potentials (Park et al., 2020b; Tabelin et al., 2017c, 2017d). In cases where the wastes contain more acid-consuming minerals like carbonates and phyllosilicates than acid-generating minerals, neutral mine drainage (NMD) contaminated with soluble heavy metal(loid)s is formed. Similarly, stockpiled leaching residues can also pollute soil as well as groundwater with toxic elements (Han et al., 2014; Silwamba et al., 2020a, 2020b).

In tailings storage facilities (TSFs), there are various arsenic (As)-bearing minerals (e.g., arsenopyrite, arsenian pyrite ($Fe(S,As)_2$), realgar (As_4S_4), orpiment (As_2S_3), etc.), so AMD with elevated concentrations of As (from < 1 μg/L to 340,000 μg/L) is often generated (Cheng et al., 2009; Park et al., 2018b, 2021; Plumlee et al., 1999). Arsenic is one of the most toxic substances because of (i) its acute toxicity at high concentrations causing nausea, vomiting, abdominal pain, and severe diarrhea, and (ii) chronic toxicity caused by long-term and repeated exposure to As at low concentrations (e.g., As-contaminated drinking water) that increases the risks of developing cancers of the skin, lungs, kidney and liver (Hughes, 2002; Park et al., 2018a; Ratnaike, 2003; Tabelin et al., 2020, 2018, 2017a, 2017b). Because of this, the Environmental Protection Agency (EPA) and the World Health Organization (WHO) lowered the maximum contaminant level (MCL) for As in drinking water from 50 μg/L to 10 μg/L (USEPA, 2001; WHO, 2018).

In order to reduce the concentration of As in AMD, there have developed numerous techniques such as oxidation, precipitation/coprecipitation, coagulation/flocculation, adsorption, ion exchange, membrane filtration, photocatalytic reduction, etc. (Levy et al., 2012; Majidnia and Fulazzaky, 2017; Mohan and Pittman, 2007;

Nicomel et al., 2016). Among them, the most commonly used technique is lime neutralization whereby the pH of AMD is raised to neutral-alkaline conditions to induce As(V) adsorption onto iron-oxyhydroxide like ferrihydrite and/or coprecipitation with ferric ions in the form of poorly crystalline ferric arsenate at Fe(III)/As(V) molar ratio ≥ 3 (De Klerk et al., 2012; Gomez et al., 2010; Jia and Demopoulos, 2008). Although this technique can lower As concentration to sub-ppm level, the generated ferric arsenate is not suitable for As control in mine effluents due to its relatively high solubility (i.e., about 25–35 mg/L As released at pH 2–5 for 24 h) (Paktunc and Bruggeman, 2010). Because of this, there have been many studies to immobilize As as scorodite ($FeAsO_4 \cdot 2H_2O$), an iron arsenate mineral with low solubility in a wide pH range (Dutrizac and Jambor, 1988; Paktunc and Bruggeman, 2010; Tabelin et al., 2019). According to solubility tests conducted by Paktunc and Bruggeman (Paktunc and Bruggeman, 2010), scorodite was stable at the pH range of 2–5 where 0.24–0.58 mg/L As was released after 9 days of testing, which is lower than EPA TCLP test limit of 5 mg/L (Bluteau and Demopoulos, 2007); however, its solubility was high at pH < 2 (20.8 mg/L As released at pH 1) and > 6 (5.38 mg/L As released at pH 7).

Precipitated scorodite, including its amorphous precursors like ferric arsenate and As-bearing ferrihydrite, produced by lime neutralization of As-rich AMDs (> 600 mg/L) are typically disposed of in special sludge disposal sites or landfills along with gypsum ($CaSO_4 \cdot 2H_2O$) (Bluteau et al., 2009). In gypsum-saturated system, the transformation of poorly crystalline ferric arsenate and crystalline scorodite to yukonite ($Ca_2Fe_{3-5}(AsO_4)_3(OH)_{4-10} \cdot xH_2O$; where x = 2–11) is well documented (Bluteau et al., 2009; Gomez et al., 2010; Jia and Demopoulos, 2008). This indicates that in special sludge disposal sites or landfills containing gypsum, Ca–Fe–AsO_4 compounds like yukonite are more stable and more suitable for As immobilization than scorodite and its amorphous precursors.

The formation of stable Ca–Fe–AsO_4 compounds, however, has only been achieved at high concentrations of As (1.4–12.8 g/L) (Bohan et al., 2014; Gomez et al., 2010; Jia and Demopoulos, 2008), so its synthesis from dilute As solution (~10 mg/L) remains challenging. In this study, As immobilization from dilute solution via a two-step process consisting of (i) concentration of As from dilute solution using schwertmannite ($Fe_8O_8(OH)_{8-2x}(SO_4)_x$; where ($1 \leq x \leq 1.75$)), and (ii) formation of Ca–Fe–AsO_4 compounds was investigated. Concentration of As from dilute solution was achieved by sorption/desorption of As(V) using schwertmannite, which was chosen because of its wide occurrence in acid-sulfate systems like AMD streams as well as its strong affinity for As (Acero et al., 2006; Burton et al., 2008; HoungAloune et al., 2015, 2014). Meanwhile, the synthesis of Ca–Fe–AsO_4 compounds was investigated under various conditions like synthesis time, temperature, and pH, and As retention abilities of the synthesized products were tested under various pH conditions.

2. Materials and Methods

2.1. Schwertmannite synthesis

Schwertmannite was synthesized using the method of HoungAloune et al. (HoungAloune et al., 2015, 2014). 500 mL solution containing 10 mM H_2SO_4 (Wako Pure Chemical Industries, Ltd., Osaka, Japan) and 50 mM $Fe_2(SO_4)_3 \cdot nH_2O$ (Wako Pure Chemical Industries, Ltd., Osaka, Japan) was prepared and heated to 65 °C while stirring at 350 rpm. Once solution temperature reached 65 °C, magnetic stirring was stopped, and the solution was titrated with 1 M Na_2CO_3 (titration rate, 1500 μL/min) until the final pH of solution reached 3–4. Afterwards, the precipitates were collected by decantation, rinsed with deionized (DI) water 5 times to remove remaining soluble ions, filtered through 5A filter paper, and dried in a vacuum oven at 40 °C for 24 h. The synthesized product was characterized by X-ray powder diffraction (XRD, MultiFlex, Rigaku Corporation, Tokyo, Japan). Moreover, the zeta potential distribution of schwertmannite as a function of pH was measured using Nano-ZS60 (Malvern Instruments, UK).

2.2. Arsenic sorption/desorption experiments for concentration of arsenic from dilute solution

For the As sorption tests, stock solutions were prepared using $Na_2HAs^{(V)}O_4 \cdot 7H_2O$ (Wako Pure Chemical Industries, Ltd., Osaka, Japan). In 100-mL Erlenmeyer flask, 50 mg of synthesized schwertmannite and 50 mL of arsenate solution were put and shaken in a constant temperature (25 °C) water bath shaker at 120 min^{-1} under various conditions: initial pH, 1.4–12.5; initial As concentration (C_i), 0.15–3.00 mM; contact time, 1–1440 min. At predetermined time intervals, suspensions were collected and filtered through 0.2 μm membrane filters, and filtrates were analyzed by inductively coupled plasma atomic emission spectrometer (ICP-AES, ICPE9820, Shimadzu Corporation, Kyoto, Japan) to measure the remaining arsenic in solution (margin of error = ±2%).

For the As desorption tests, 50 mg of As-loaded schwertmannite (As-sch), prepared by reacting 50 mg of schwertmannite with 50 mL of arsenate solution (0.15 mM) at pH 3 for 24 h, was mixed with 5 mL of NaOH solution (pH 13) in a water bath shaker at 25 °C and 120 min^{-1} for 1–1440 min, and the content of arsenic desorbed was determined by ICP-AES.

Concentration of dilute As solution (0.15 mM ≈ 11.2 mg/L) was conducted via As sorption from a large volume (V_i = 50–250 mL) of As-containing solution at pH 3 using 0.1 g of schwertmannite followed by As desorption from 0.1 g of As-sch into a small volume (V_f = 5 mL) of pH 13 solution, i.e., volume ratios of solutions for sorption and desorption were varied from 10 to 50. Arsenic concentrations in solutions before (C_i) and after concentration (C_f) were measured by ICP-AES to calculate the concentration ratio (C_f/C_i).

To check the recyclability of schwertmannite, the As concentration process—a combination of sorption (M_{sch},

50 mg; C_i, 0.15 mM; V_i, 50 mL; pH, 3; time, 24 h; temp., 25 °C) and desorption ($M_{As\text{-}sch}$, 50 mg; V_f, 5 mL; pH, 13; time, 24 h; temp., 25 °C)—was repeated 4 times and concentration ratios (C_f/C_i) were compared. Moreover, schwertmannite samples before and after 4 cycles of concentration were characterized by XRD.

2.3. Immobilization of arsenic via synthesis of Ca-Fe-AsO_4 compounds

The synthesis of Ca-Fe-AsO_4 compounds was carried out based on the procedure developed by Becze and Demopoulos (Becze and Demopoulos, 2007). In 2 g/L As(V) solution, $Fe_2(SO_4)_3 \cdot 5H_2O$ (Acros Organics, Geel, Belgium) and $CaSO_4 \cdot 2H_2O$ (Wako Pure Chemical Industries, Ltd., Osaka, Japan) were added to adjust Ca/Fe/As molar ratio to 0.5/0.75/1.0. After this, solution pH was adjusted to the desired value (pH 8, 10, and 12) using 1 M NaOH and heated to 25–95 °C for 24–72 h while stirring at 300 rpm. The detailed conditions for synthesis were summarized in Table 1. The synthesized products were collected by filtration using 5A filter paper, rinsed with DI water 5 times, dried in a vacuum oven at 40 °C for 24 h, and characterized by XRD.

To check the stabilities of Ca-Fe-AsO_4 compounds synthesized at pH 8 and 12, they were leached with solutions (pH 1–12) at pulp density of 0.1 g/ 10 mL for 24 h in a water bath shaker (25 °C) at 120 min^{-1}. For comparison, the same leaching experiment was conducted for As-loaded schwertmannite. After 24 h, suspensions were filtered through 0.2 μm syringe-driven membrane filters, and filtrates were analyzed by ICP-AES. All chemicals used in this study were of reagent grade.

Table 1. A summary of conditions for the synthesis of Ca-Fe-AsO_4 compounds.

	Initial As(V) conc.	Ca/Fe/As molar ratio	Synthesis time	Temperature	pH
Case 1	2 g/L	0.5/0.75/1.0	24 h	95 °C	8
Case 2			48 h	95 °C	8
Case 3			72 h	95 °C	8
Case 4			24 h	25 °C	8
Case 5			24 h	50 °C	8
Case 6			24 h	75 °C	8
Case 7			24 h	95 °C	10
Case 8			24 h	95 °C	12

3. Results and Discussion

3.1. Arsenic sorption/desorption using schwertmannite

Figure 1a shows As sorption to schwertmannite as a function of pH. Arsenic sorption to schwertmannite was strongly pH-dependent and ranged between ~5% and ~99%. Under strongly acidic conditions (pH 1.3), As sorption was only < 5%. This low sorption of arsenate to schwertmannite is most likely due to its neutral species (i.e., H_3AsO_4; Fig. 1b) that is less attracted to a positively-charged sorbent than anionic species like $H_2AsO_3^-$ and

$HAsO_3^{2-}$. Moreover, instability of schwertmannite at pH < 2 could be another reason for low As sorption (Caraballo et al., 2013; HoungAloune et al., 2015; Smedley and Kinniburgh, 2002). At initial pH of 2.0–9.2, arsenate adsorption onto schwertmannite dramatically improved and reached 90–99%. When arsenate was adsorbed at initial pH of 3.0–9.2, the final pH decreased to pH 2.8–3.4, indicating that As(V) anionic species (e.g., $H_2AsO_3^-$ and $HAsO_3^{2-}$) were deprotonated and adsorbed via oxyanion-sulfate exchange reactions (Antelo et al., 2012). As pH increased to > 12, As sorption decreased dramatically to ~20%. The isoelectric point (IEP) of schwertmannite was measured to be ~8.4 (Fig. 1c), which means that at pH > IEP, schwertmannite is negatively charged (i.e., ≡Fe–O^-; ≡ indicates the surface of schwertmannite). Under these conditions, repulsion between schwertmannite and arsenate present as the fully deprotonated form (AsO_4^{3-}) is greater, which made As sorption to schwertmannite inefficient (Burton et al., 2009; Dou et al., 2013; HoungAloune et al., 2015).

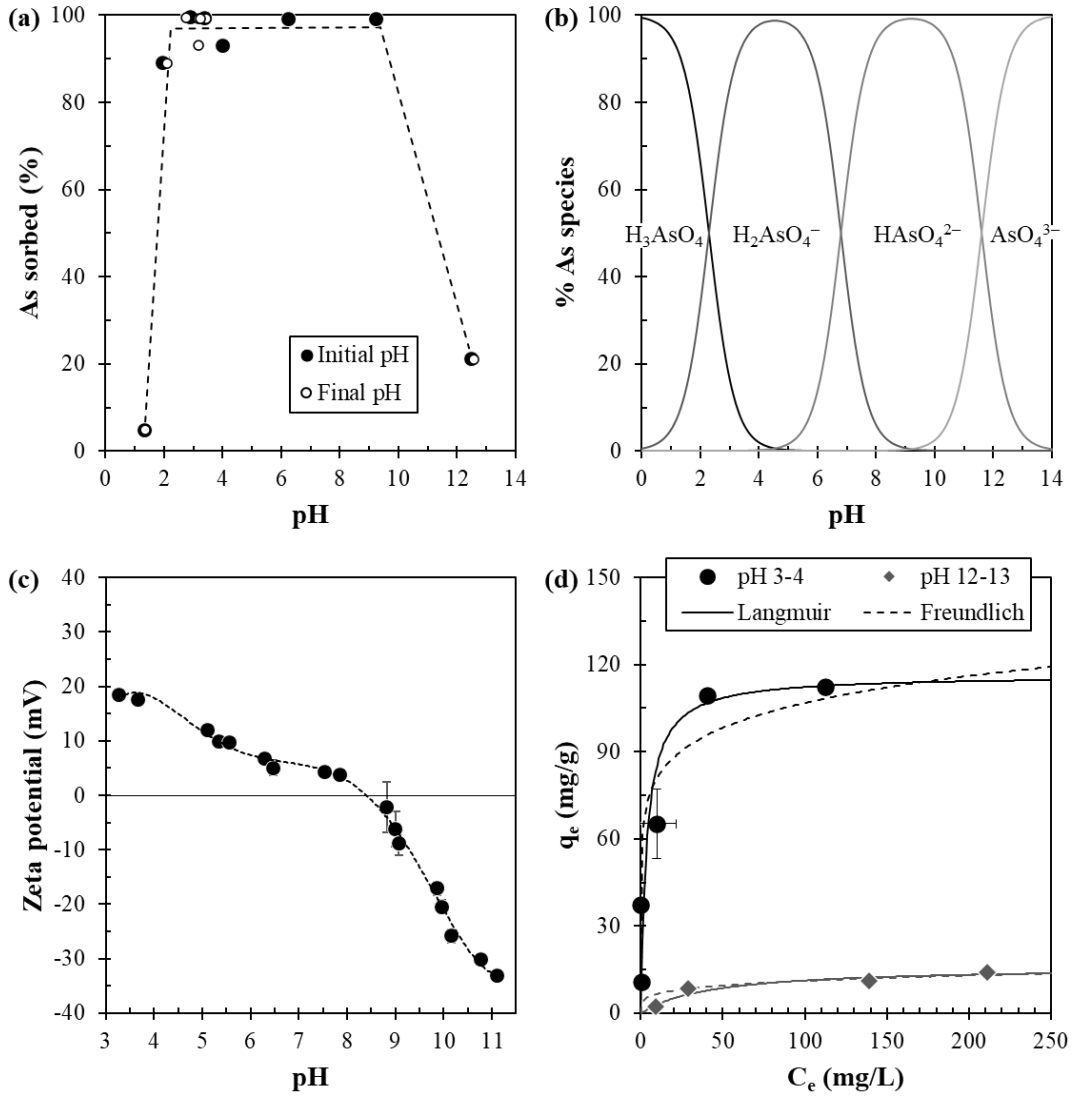

Figure 1. (a) As sorption to schwertmannite as a function of pH, (b) speciation diagram of arsenate from pH 0 to 14, (c) zeta potential of schwertmannite, and (d) equilibrium isotherm models for As(V) sorption on schwertmannite at pH 3 and 13.

Adsorption isotherms of arsenate at pH 3 and 13 are illustrated in Fig. 1d. Equilibrium sorption data were fitted with Langmuir (Eq. 1) and Freundlich (Eq. 2) isotherm models:

$$q_e = \frac{Q_{max} K_L C_e}{1 + K_L C_e}, \quad (1)$$

$$q_e = K_F {C_e}^n, \quad (2)$$

where q_e (mg/g) and C_e (mg/L) in Eqs. 1 and 2 are the amount of As adsorbed onto schwertmannite and the equilibrium As concentration, Q_{max} (mg/g) and K_L (L/mg) in Eq. 1 correspond to the maximum adsorption capacity and Langmuir constant, and K_F ((mg/g)/((mg/L)^n)) and n (dimensionless) in Eq. 2 represent the Freundlich constants related to adsorption capacity and adsorption intensity (Foo and Hameed, 2010; Freundlich, 1906; Ho et al., 2002; Langmuir, 1918; Tran et al., 2017). The Langmuir isotherm model assumes a monolayer sorption that occurs at a finite number of sorption sites, and Freundlich model is an empirical model allowing for multilayer sorption onto heterogeneous surfaces (Langmuir, 1918; Freundlich, 1906; Ho et al., 2002; Tran et al., 2017; Foo and Hameed, 2010). The parameters obtained from Langmuir and Freundlich isotherm models are summarized in Table 2. In addition, the adequacy of these two models for a given set of data was assessed using Akaike information criterion (AIC)—a methodology for model selection in a situation where more than one model has been fitted to data (Akaike, 1974; Akpa and Unuabonah, 2011). AIC is mathematically expressed as follows:

$$AIC = 2k + n\left[ln\left(\frac{SSR}{(n)}\right)\right], \quad (3)$$

where k and n are the number of parameters in the model and the number of data points, respectively, and SSR denotes the sum of squares for the residual. For a small number of observations (i.e., n/k < 40), the second-order Akaike information criterion (AIC_c) should be used instead of AIC (Cao et al., 2021; Elnakar and Buchanan, 2020; Hurvich and Tsai, 1989; Rajahmundry et al., 2021):

$$AIC_c = AIC + \left[\frac{2k(k+1)}{n-k-1}\right] \quad (4)$$

The best model within the collection of models considered given the data is the one with the minimum AIC_c value (Portet, 2020). As can be seen in Table 2, AIC_c value for Langmuir isotherm model is lower than that for Freundlich isotherm model, which indicate that the former fitted the experimental data better than the latter. The maximum As sorption capacities at pH 3 and 13 calculated by Langmuir isotherm (Q_{max}) were 116.3 and 16.1 mg/g, respectively. Arsenate sorption capacities of schwertmannite measured in other works are summarized in Table 3.

Table 2. Langmuir and Freundlich isotherm constants.

Isotherm model	Parameter	pH 3	pH 13
Langmuir	Q_{max}	116.3	16.1
	K_L	0.28	0.02
	R^2	0.99	0.97
	AIC_c	–28.5	15.7
Freundlich	K_F	61.4	5.86
	n	0.12	0.16
	R^2	0.92	0.91
	AIC_c	–0.4	35.8

Table 3. A comparison of As(V) sorption capacity of natural and synthesized schwertmannite.

Schwertmannite	Adsorbent dose (g/L)	pH	Time (h)	Temp. (ºC)	As(V) sorption capacity (mg/g)	Ref.
Natural	–	–	–	–	60.9	Fukushi et al. (2013)
Natural	–	–	–	–	69.8	Carlson et al. (2002)
Synthesized	0.3	5.0	24	25	104.2	Dou et al. (2013)
Synthesized	1.0	4.0	24	25	82.4	Fukushi et al. (2004)
Synthesized	1.0	3–4	24	25	114.0	HoungAloune et al. (2014)
Synthesized	1.0	3.0	24	25	116.3	This study
	1.0	13.0	24	25	16.1	

Figure 2 shows As sorption to schwertmannite and As desorption from As-loaded schwertmannite with time. As confirmed by Fig. 1, As sorption to schwertmannite occurred favorably under acidic conditions whereas its sorption was limited under alkaline conditions, and thus As sorption and desorption were conducted at pH 3 and 13, respectively. As shown in Fig. 2a, As sorption reached > 99% within 10 min of contact time and remained unchanged up to 24 h. Similarly, As desorption reached apparent equilibrium after 10 min and ranged between 57% and 66% (Fig. 2b). Although both sorption and desorption reached equilibrium within 10 min, contact times for the succeeding sorption and desorption tests were fixed at 24 h to allow the system to reach equilibrium.

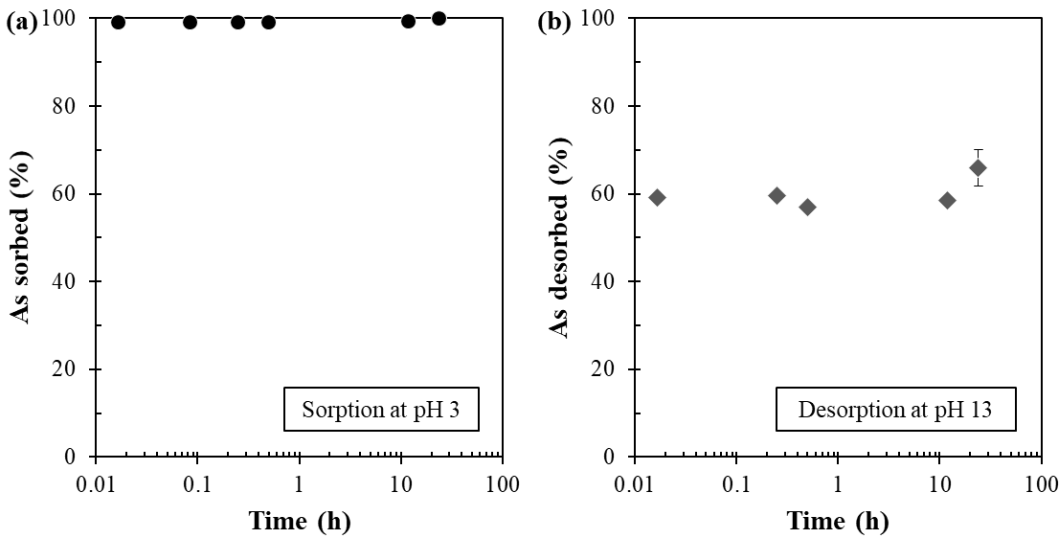

Figure 2. (a) Arsenic sorption to schwertmannite at pH 3, and (b) desorption from As-loaded schwertmannite at pH 13 with time.

3.2. Concentration of arsenic from dilute solution

Concentration of As from dilute solution ($[As(V)]_{initial}$ = 0.15 mM ≈ 11.2 mg/L) via As sorption with large volume of As-containing solution (V_i) followed by As desorption with small volume of eluent (V_f) was investigated at various V_i/V_f ratio. Figure 3a shows initial (C_i) and final (C_f) As concentration as well as their ratio (i.e., C_f/C_i; an indicator how much As is concentrated) obtained after 24 h sorption/desorption. With increasing V_i/V_f ratio, final As concentration increased, and concentration ratios at V_i/V_f of 10, 25, and 50 were 6, 17, and 35, respectively (Fig. 3a). The concentration ratios observed were lower than expected. During sorption, > 97% of As(V) was loaded onto schwertmannite irrespective of V_i; however, As desorption from As-sch was about 56–72%, which is the main cause of lower concentration ratios compared with expected values (e.g., $10_{exp}\rightarrow6_{obs}$; $25_{exp}\rightarrow17_{obs;}$ $50_{exp}\rightarrow35_{obs}$). Although desorption was incomplete, the results confirmed that sorption/desorption using schwertmannite can be utilized for concentrating As from dilute solutions.

Concentration ratio of As under the given conditions can be mathematically calculated. A mass balance equation during sorption is expressed as follows:

$$M_{sch}q_{e,A} = V_iC_i - V_iC_{e,A}, \quad (5)$$

where M_{sch}, V_i, and C_i denote mass of schwertmannite (g), initial volume of As solution (L), and initial concentration of As (mg/L), respectively, while $q_{e,A}$ and $C_{e,A}$ represent the amount of As loaded onto

schwertmannite (mg/g) and equilibrium As concentration (mg/L) after sorption finished. By incorporating the Langmuir isotherm (Eq. 6) into Eq. 5, a quadratic equation for $C_{e,A}$ (Eq. 7) is produced.

$$q_{e,A} = \frac{Q_{max} K_L C_{e,A}}{1 + K_L C_{e,A}}, \quad (6)$$

$$V_i K_L C_{e,A}^2 + (M_{sch} Q_{max} K_L - V_i K_L C_i + V_i) C_{e,A} - V_i C_i = 0, \quad (7)$$

where Q_{max} and K_L are Langmuir isotherm constants obtained at pH 3 (Table 2). By solving Eq. 7 through a quadratic formula, $C_{e,A}$ can be calculated and used for calculating $q_{e,A}$. Meanwhile, a mass balance equation during desorption is expressed as follows:

$$C_f V_f = M_{sch} q_{e,A} - M_{As-sch} q_{e,D}, \quad (8)$$

where $M_{As\text{-}sch}$, V_f, and C_f denote mass of As-loaded schwertmannite (g), volume of eluent (L), and final concentration of As (mg/L), respectively, while $q_{e,D}$ and $C_{e,D}$ represent the amount of As remained as sorbed on schwertmannite (mg/g) and equilibrium As concentration (mg/L) after desorption finished. Similarly, by incorporating the Langmuir isotherm (Eq. 9) into Eq. 8, a quadratic equation for C_f (Eq. 10) is produced:

$$q_{e,D} = \frac{Q_{max} K_L C_{e,D}}{1 + K_L C_{e,D}}, \quad (9)$$

$$V_f K_L C_f^2 + \left(V_f - M_{sch} q_{e,A} K_L + M_{As-sch} Q_{max} K_L\right) C_f - M_{sch} q_{e,A} = 0, \quad (10)$$

where Q_{max} and K_L are Langmuir isotherm constants obtained at pH 13, and $C_{e,D}$ is equilibrium As concentration (mg/L) after desorption finished, which is equal to C_f (i.e., $C_{e,D} = C_f - C_i = C_f$ because $C_i = 0$). Therefore, C_f can be calculated via a quadratic formula of Eq. 10.

Figure 3b shows an example of estimation of concentration ratio under the following conditions: C_i, 0.15 mM; M_{sch}, 50, 250, 500 mg; V_i, 0.025–2.5L; V_f, 0.005 L. As can be seen, concentration ratio increases with increasing V_f/V_i ratio, and higher concentration ratio can be achieved by increasing the amount of schwertmannite. To concentrate dilute As solution (C_i = 0.15 mM ≈ 11.2 mg/L) to > 2000 mg/L, sorption/desorption at V_i/V_f ratio of > 350 (M_{sch}/V_f = 50 g/L) and > 370(M_{sch}/V_f = 100 g/L) is required.

As sorption/desorption was repeated 4 times to check the recyclability of schwertmannite for As concentration. As illustrated in Fig. 4a, concentration ratios were similar regardless of cycle numbers (i.e., C_f/C_i = 6.9 ± 0.5). Moreover, XRD patterns of schwertmannite before and after 4 cycles of sorption/desorption process show that schwertmannite was not degraded even after being used repeatedly (Fig. 4b). These results indicate that schwertmannite can be used for concentrating As from dilute solution, and after As desorption, it can be reutilized as As sorbent.

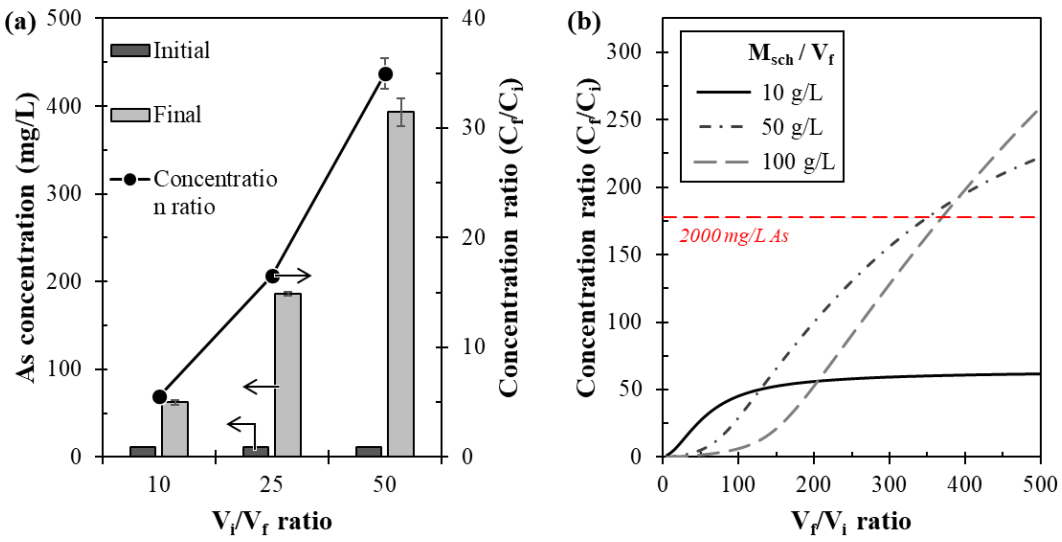

Figure 3. (a) Arsenic concentration before and after concentration via sorption of arsenate from As(V)-containing solution (volume: V_i) at pH 3 using schwertmannite and desorption of arsenate from As-loaded schwertmannite using pH 13 solution (volume: V_f), and (b) Theoretical calculation of concentration ratio as a function of V_f/V_i ratio.

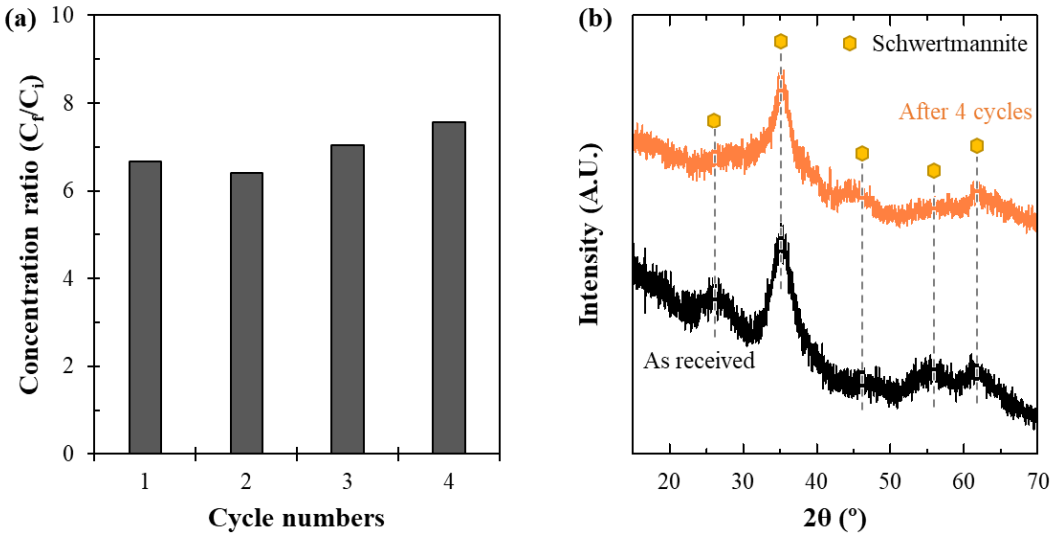

Figure 4. Recyclability of schwertmannite for arsenic concentration: (a) effects of cycle numbers on the concentration ratio of arsenate, and (b) XRD patterns of schwertmannite before and after 4 cycles.

3.3. Synthesis of Ca-Fe-AsO$_4$ compounds from concentrated As solution

Figures 5a–c show XRD patterns of synthesized products (Case 1–8). As shown in Fig. 5a, yukonite ($Ca_2Fe_{3-5}(AsO_4)_3(OH)_{4-10}\cdot xH_2O$; where x =2–11) (Gomez et al., 2010) was synthesized from 2 g/L As(V) solution in the presence of Ca^{2+} and Fe^{3+} (Ca:Fe:As = 0.5:0.75:1.0) at 95 °C and pH 8 within 24 h. Meanwhile, mineralogical

compositions of synthesized products were greatly affected by temperature (Fig. 5b). At low temperature (25–50 °C), poorly crystalline ferric arsenate ($FeAsO_4 \cdot 2.4H_2O$) (Jia et al., 2007, 2006) was formed. At 75 °C, yukonite was formed together with poorly crystalline ferric arsenate, and at 95 °C, only yukonite was synthesized (Fig. 5b). Similarly, pH was also one of the most important parameters for determining mineralogical compositions of synthesized products. As shown in Fig. 5c, yukonite was formed at pH 8 but was unstable at pH 10, resulting in the formation of ferric arsenate. At pH 12, a new mineral was formed, johnbaumite ($Ca_5(AsO_4)_3OH$) (Puzio et al., 2018; Zhang et al., 2019), together with goethite (α-FeOOH) (Vithana et al., 2015).

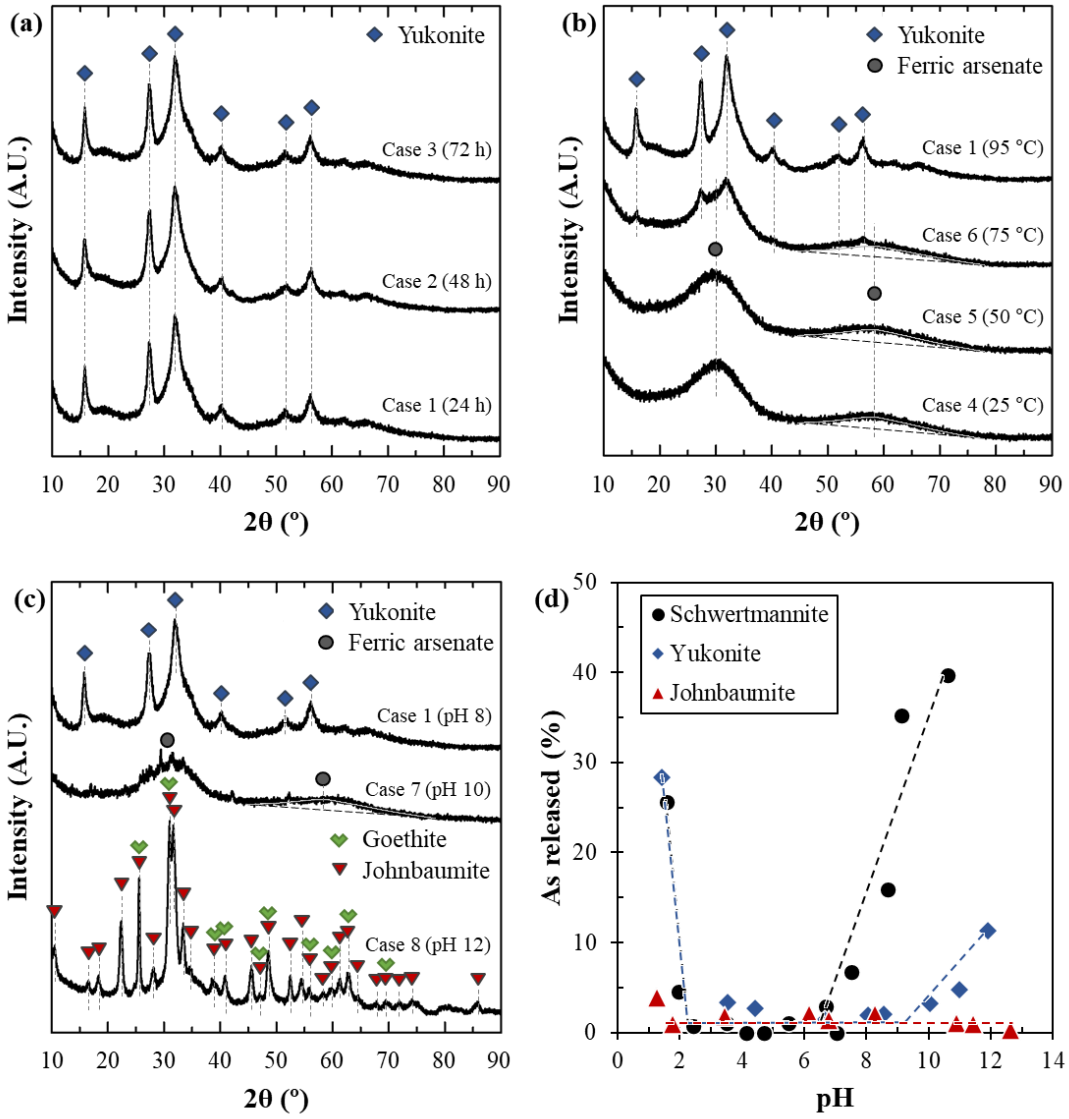

Figure 5. XRD patterns of synthesized products at various (a) synthesis time, (b) temperature, and (c) pH, and (d) the release of arsenic from As-loaded schwertmannite, yukonite (Case 1), and johnbaumite (Case 8) as a function of pH.

To check the As retention abilities of schwertmannite, yukonite (Case 1), and johnbaumite (Case 8), they were leached at various pH conditions (pH 1.2–12.6) (Fig. 5d). Both schwertmannite and yukonite were ineffective to immobilize As under strongly acidic conditions (< pH 2), while johnbaumite was able to retain As even at pH < 2. Under neutral to alkaline conditions, As started being released from schwertmannite and yukonite at pH > 6.5 and 9, respectively; however, very little As was released from johnbaumite. Moreover, As desorption was done at pH 12–13, so the synthesis of johnbaumite is beneficial in terms of pH regulation compared to yukonite. Therefore, among the three minerals tested, johnbaumite is the most promising to immobilize As.

Figure 6 shows the proposed scheme for treating As-contaminated mine drainage. For the case that either influent pH is lower than 2 or arsenite (As^{III}) is present, a neutralization using lime with aeration is required for increasing its pH to ~3 as well as oxidizing As^{III} to As^{V} prior to the sorption process. Afterward, mine drainage is passed through a packed-bed reactor filled with schwertmannite, resulting in the sorption of almost all As^{V} on the sorbent.

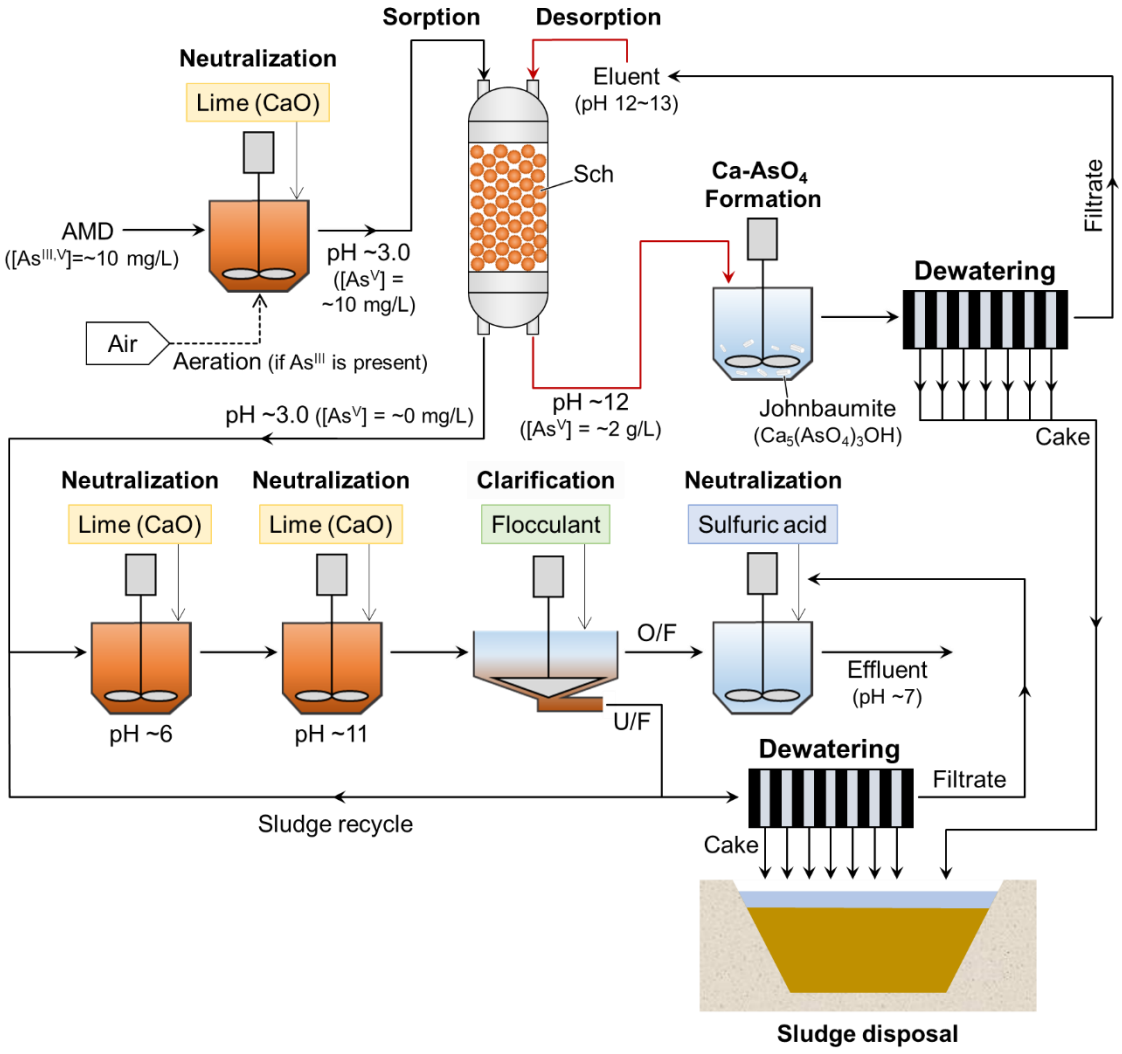

Figure 6. A proposed scheme for treating As-contaminated mine drainage.

After the sorption process, a small volume of eluent solution (pH 12–13 adjusted by lime) is introduced to a packed-bed reactor for producing As^V-concentrated solution ([As^V] = ~2 g/L), which is transferred to the process in which calcium arsenate like johnbaumite ($Ca_5(AsO_4)_3OH$) is generated. The suspension is then dewatered by filter press, and the obtained sludge cakes are disposed of into the sludge disposal dam while filtrates are reutilized as eluents. Meanwhile, effluents obtained after sorption process are still acidic and contain elevated levels of heavy metals, which need to be treated appropriately to meet the effluent discharge limits. To this end, the application of high density sludge (HDS) process—a modification of the active lime treatment process where a portion of the settled solids from the clarifier (i.e., sludge) is recycled and mixed with fresh lime prior to contact with AMD (Mackie and Walsh, 2015)—is recommended.

4. Conclusions

This study investigated a novel As immobilization by the combination of sorption/desorption-based concentration of As from dilute solution using schwertmannite and synthesis of stable As-bearing mineral under alkaline conditions. Arsenic sorption to schwertmannite was pH dependent and favored at a pH range of 2–9 while it was limited at pH < 2 and > 9. Between Freundlich and Langmuir isotherm models, the experimental data were fitted well with the latter as its AICc value was lower than that of the former. The maximum sorption capacities for As(V) were 116.3 mg/g at pH 3 and 16.1 mg/g at pH 13, which facilitated As concentration via sorption at pH 3 with large volume of dilute solution followed by desorption at pH 13 with small volume of eluent. To concentrate As(V) from 11.2 to 2000 mg/L, it was estimated that sorption using 50 g of schwertmannite in 350 L of As(V) solution and desorption in 1 L of eluent are required. From As(V) concentrate (2000 mg/L), amorphous ferric arsenate was formed at low temperature (25–50 °C), whereas high temperature (~95 °C) favored the production of yukonite (at pH 8) and johnbaumite (at pH 12). Among the synthesized products (As-loaded schwertmannite, johnbaumite, and yukonite), johnbaumite was the most promising compound for immobilizing As due to its exceptional As retention ability compared to those of schwertmannite and yukonite.

References

Acero, P., Ayora, C., Torrentó, C., Nieto, J.-M., 2006. The behavior of trace elements during schwertmannite precipitation and subsequent transformation into goethite and jarosite. Geochim. Cosmochim. Acta 70, 4130–4139. https://doi.org/10.1016/j.gca.2006.06.1367

Akaike, H., 1974. A new look at the statistical model identification. IEEE Trans. Autom. Control 19, 716–723.

https://doi.org/10.1109/TAC.1974.1100705

Akpa, O.M., Unuabonah, E.I., 2011. Small-Sample Corrected Akaike Information Criterion: An appropriate statistical tool for ranking of adsorption isotherm models. Desalination 272, 20–26. https://doi.org/10.1016/j.desal.2010.12.057

Antelo, J., Fiol, S., Gondar, D., López, R., Arce, F., 2012. Comparison of arsenate, chromate and molybdate binding on schwertmannite: Surface adsorption vs anion-exchange. J. Colloid Interface Sci. 386, 338–343. https://doi.org/10.1016/j.jcis.2012.07.008

Becze, L., Demopoulos, G.P., 2007. Hydrometallurgical synthesis, characterization and stability of Ca-Fe-AsO_4 compounds, in: Extraction and Processing Proceedings. TMS, Warrendale, PA, pp. 11–17.

Bluteau, M.-C., Becze, L., Demopoulos, G.P., 2009. The dissolution of scorodite in gypsum-saturated waters: Evidence of Ca–Fe–AsO4 mineral formation and its impact on arsenic retention. Hydrometallurgy 97, 221–227. https://doi.org/10.1016/j.hydromet.2009.03.009

Bluteau, M.-C., Demopoulos, G.P., 2007. The incongruent dissolution of scorodite — Solubility, kinetics and mechanism. Hydrometallurgy 87, 163–177. https://doi.org/10.1016/j.hydromet.2007.03.003

Bohan, M.T., Mahoney, J.J., Demopoulos, G.P., 2014. The Synthesis and Stability of Yukonite: Implications in Solid Arsenical Waste Storage, in: Rare Metal Technology 2014. TMS, Warrendale, PA, U.S.A., pp. 9–10.

Burton, E.D., Bush, R.T., Johnston, S.G., Watling, K.M., Hocking, R.K., Sullivan, L.A., Parker, G.K., 2009. Sorption of Arsenic(V) and Arsenic(III) to Schwertmannite. Environ. Sci. Technol. 43, 9202–9207. https://doi.org/10.1021/es902461x

Burton, E.D., Bush, R.T., Sullivan, L.A., Mitchell, D.R.G., 2008. Schwertmannite transformation to goethite via the Fe(II) pathway: Reaction rates and implications for iron–sulfide formation. Geochim. Cosmochim. Acta 72, 4551–4564. https://doi.org/10.1016/j.gca.2008.06.019

Cao, Y., Dong, S., Dai, Z., Zhu, L., Xiao, T., Zhang, X., Yin, S., Soltanian, M.R., 2021. Adsorption model identification for chromium (VI) transport in unconsolidated sediments. J. Hydrol. 598, 126228. https://doi.org/10.1016/j.jhydrol.2021.126228

Caraballo, M.A., Rimstidt, J.D., Macías, F., Nieto, J.M., Hochella, M.F., 2013. Metastability, nanocrystallinity and pseudo-solid solution effects on the understanding of schwertmannite solubility. Chem. Geol. 360–361, 22–31. https://doi.org/10.1016/j.chemgeo.2013.09.023

Carlson, L., Bigham, J.M., Schwertmann, U., Kyek, A., Wagner, F., 2002. Scavenging of As from Acid Mine

Drainage by Schwertmannite and Ferrihydrite: A Comparison with Synthetic Analogues. Environ. Sci. Technol. 36(8), 1712–1719. https://doi.org/10.1021/es0110271

Cheng, H., Hu, Y., Luo, J., Xu, B., Zhao, J., 2009. Geochemical processes controlling fate and transport of arsenic in acid mine drainage (AMD) and natural systems. J. Hazard. Mater. 165, 13–26. https://doi.org/10.1016/j.jhazmat.2008.10.070

De Klerk, R.J., Jia, Y., Daenzer, R., Gomez, M.A., Demopoulos, G.P., 2012. Continuous circuit coprecipitation of arsenic(V) with ferric iron by lime neutralization: Process parameter effects on arsenic removal and precipitate quality. Hydrometallurgy 111–112, 65–72. https://doi.org/10.1016/j.hydromet.2011.10.004

Dou, X., Mohan, D., Pittman, C.U., 2013. Arsenate adsorption on three types of granular schwertmannite. Water Res. 47, 2938–2948. https://doi.org/10.1016/j.watres.2013.01.035

Dutrizac, J.E., Jambor, J.L., 1988. The synthesis of crystalline scorodite, FeAsO4 · 2H2O. Hydrometallurgy 19, 377–384. https://doi.org/10.1016/0304-386X(88)90042-4

Elnakar, H., Buchanan, I., 2020. Soluble chemical oxygen demand removal from bypass wastewater using iron electrocoagulation. Sci. Total Environ. 706, 136076. https://doi.org/10.1016/j.scitotenv.2019.136076

Foo, K.Y., Hameed, B.H., 2010. Insights into the modeling of adsorption isotherm systems. Chem. Eng. J. 156, 2–10. https://doi.org/10.1016/j.cej.2009.09.013

Freundlich, H.M.F., 1906. Über die Adsorption in Lösungen. Z. Für Phys. Chem. 57, 385–470. https://doi.org/10.1515/zpch-1907-5723

Fukushi, K., Sasaki, M., Sato, T., Yanase, N., Amano, H., Ikeda, H., 2003. A natural attenuation of arsenic in drainage from an abandoned arsenic mine dump. Appl. Geochem. 18(8), 1267–1278. https://doi.org/10.1016/S0883-2927(03)00011-8

Fukushi, K., Sato, T., Yanase, N., Minato, J., Yamada, H., 2004. Arsenate sorption on schwertmannite. Am. Mineral. 89, 1728–1734. https://doi.org/10.2138/am-2004-11-1219

Gomez, M.A., Becze, L., Blyth, R.I.R., Cutler, J.N., Demopoulos, G.P., 2010. Molecular and structural investigation of yukonite (synthetic & natural) and its relation to arseniosiderite. Geochim. Cosmochim. Acta 74, 5835–5851. https://doi.org/10.1016/j.gca.2010.07.023

Han, H., Sun, W., Hu, Y., Jia, B., Tang, H., 2014. Anglesite and silver recovery from jarosite residues through roasting and sulfidization-flotation in zinc hydrometallurgy. J. Hazard. Mater. 278, 49–54. https://doi.org/10.1016/j.jhazmat.2014.05.091

Ho, Y.S., Porter, J.F., McKay, G., 2002. Equilibrium Isotherm Studies for the Sorption of Divalent Metal Ions onto

Peat: Copper, Nickel and Lead Single Component Systems. Water. Air. Soil Pollut. 141, 1–33. https://doi.org/10.1023/A:1021304828010

HoungAloune, S., Hiroyoshi, N., Ito, M., 2015. Stability of As(V)-sorbed schwertmannite under porphyry copper mine conditions. Miner. Eng. 74, 51–59. https://doi.org/10.1016/j.mineng.2015.01.003

HoungAloune, S., Kawaai, T., Hiroyoshi, N., Ito, M., 2014. Study on schwertmannite production from copper heap leach solutions and its efficiency in arsenic removal from acidic sulfate solutions. Hydrometallurgy 147–148, 30–40. https://doi.org/10.1016/j.hydromet.2014.04.001

Hughes, M.F., 2002. Arsenic toxicity and potential mechanisms of action. Toxicol. Lett. 133, 1–16. https://doi.org/10.1016/S0378-4274(02)00084-X

Hurvich, C.M., Tsai, C.-L., 1989. Regression and time series model selection in small samples. Biometrika 76, 297–307. https://doi.org/10.1093/biomet/76.2.297

Jia, Y., Demopoulos, G.P., 2008. Coprecipitation of arsenate with iron(III) in aqueous sulfate media: Effect of time, lime as base and co-ions on arsenic retention. Water Res. 42, 661–668. https://doi.org/10.1016/j.watres.2007.08.017

Jia, Y., Xu, L., Fang, Z., Demopoulos, G.P., 2006. Observation of Surface Precipitation of Arsenate on Ferrihydrite. Environ. Sci. Technol. 40, 3248–3253. https://doi.org/10.1021/es051872+

Jia, Y., Xu, L., Wang, X., Demopoulos, G.P., 2007. Infrared spectroscopic and X-ray diffraction characterization of the nature of adsorbed arsenate on ferrihydrite. Geochim. Cosmochim. Acta 71, 1643–1654. https://doi.org/10.1016/j.gca.2006.12.021

Langmuir, I., 1918. THE ADSORPTION OF GASES ON PLANE SURFACES OF GLASS, MICA AND PLATINUM. J. Am. Chem. Soc. 40, 1361–1403. https://doi.org/10.1021/ja02242a004

Levy, I.K., Mizrahi, M., Ruano, G., Zampieri, G., Requejo, F.G., Litter, M.I., 2012. TiO2-Photocatalytic Reduction of Pentavalent and Trivalent Arsenic: Production of Elemental Arsenic and Arsine. Environ. Sci. Technol. 46, 2299–2308. https://doi.org/10.1021/es202638c

Mackie, A.L., Walsh, M.E., 2015. Investigation into the use of cement kiln dust in high density sludge (HDS) treatment of acid mine water. Water Res. 85, 443–450. https://doi.org/10.1016/j.watres.2015.08.056

Majidnia, Z., Fulazzaky, M.A., 2017. Photocatalytic reduction of Cs(I) ions removed by combined maghemite-titania PVA-alginate beads from aqueous solution. J. Environ. Manage. 191, 219–227. https://doi.org/10.1016/j.jenvman.2017.01.019

Mohan, D., Pittman, C.U., 2007. Arsenic removal from water/wastewater using adsorbents—A critical review. J.

Hazard. Mater. 142, 1–53. https://doi.org/10.1016/j.jhazmat.2007.01.006

Nicomel, N.R., Leus, K., Folens, K., Van Der Voort, P., Du Laing, G., 2016. Technologies for Arsenic Removal from Water: Current Status and Future Perspectives. Int. J. Environ. Res. Public. Health 13, 62. https://doi.org/10.3390/ijerph13010062

Paktunc, D., Bruggeman, K., 2010. Solubility of nanocrystalline scorodite and amorphous ferric arsenate: Implications for stabilization of arsenic in mine wastes. Appl. Geochem. 25, 674–683. https://doi.org/10.1016/j.apgeochem.2010.01.021

Park, I., Tabelin, C.B., Magaribuchi, K., Seno, K., Ito, M., Hiroyoshi, N., 2018a. Suppression of the release of arsenic from arsenopyrite by carrier-microencapsulation using Ti-catechol complex. J. Hazard. Mater. 344, 322–332. https://doi.org/10.1016/j.jhazmat.2017.10.025

Park, I., Tabelin, C.B., Seno, K., Jeon, S., Ito, M., Hiroyoshi, N., 2018b. Simultaneous suppression of acid mine drainage formation and arsenic release by Carrier-microencapsulation using aluminum-catecholate complexes. Chemosphere 205, 414–425. https://doi.org/10.1016/j.chemosphere.2018.04.088

Park, I., Tabelin, C.B., Jeon, S., Li, X., Seno, K., Ito, M., Hiroyoshi, N., 2019. A review of recent strategies for acid mine drainage prevention and mine tailings recycling. Chemosphere 219, 588–606. https://doi.org/10.1016/j.chemosphere.2018.11.053

Park, I., Hong, S., Jeon, S., Ito, M., Hiroyoshi, N., 2020a. A Review of Recent Advances in Depression Techniques for Flotation Separation of Cu–Mo Sulfides in Porphyry Copper Deposits. Metals 10, 1269. https://doi.org/10.3390/met10091269

Park, I., Tabelin, C.B., Seno, K., Jeon, S., Inano, H., Ito, M., Hiroyoshi, N., 2020b. Carrier-microencapsulation of arsenopyrite using Al-catecholate complex: nature of oxidation products, effects on anodic and cathodic reactions, and coating stability under simulated weathering conditions. Heliyon 6, e03189. https://doi.org/10.1016/j.heliyon.2020.e03189

Park, I., Higuchi, K., Tabelin, C.B., Jeon, S., Ito, M., Hiroyoshi, N., 2021. Suppression of arsenopyrite oxidation by microencapsulation using ferric-catecholate complexes and phosphate. Chemosphere 269, 129413. https://doi.org/10.1016/j.chemosphere.2020.129413

Plumlee, G.S., Smith, K.S., Montour, M.R., Ficklin, W.H., Mosier, E.L., 1999. Geologic Controls on the Composition of Natural Waters and Mine Waters Draining Diverse Mineral-Deposit Types, in: The Environmental Geochemistry of Mineral Deposits. Part B, Case Studies and Research Topics. Society of Economic Geologists, Littleton, CO, pp. 373–432.

Portet, S., 2020. A primer on model selection using the Akaike Information Criterion. Infect. Dis. Model. 5, 111–128. https://doi.org/10.1016/j.idm.2019.12.010

Puzio, B., Manecki, M., Kwaśniak-Kominek, M., 2018. Transition from Endothermic to Exothermic Dissolution of Hydroxyapatite Ca5(PO4)3OH–Johnbaumite Ca5(AsO4)3OH Solid Solution Series at Temperatures Ranging from 5 to 65 °C. Minerals 8, 281. https://doi.org/10.3390/min8070281

Rajahmundry, G.K., Garlapati, C., Kumar, P.S., Alwi, R.S., Vo, D.-V.N., 2021. Statistical analysis of adsorption isotherm models and its appropriate selection. Chemosphere 276, 130176. https://doi.org/10.1016/j.chemosphere.2021.130176

Ratnaike, R.N., 2003. Acute and chronic arsenic toxicity. Postgrad. Med. J. 79, 391–396. https://doi.org/10.1136/pmj.79.933.391

Silwamba, M., Ito, M., Hiroyoshi, N., Tabelin, C.B., Fukushima, T., Park, I., Jeon, S., Igarashi, T., Sato, T., Nyambe, I., Chirwa, M., Banda, K., Nakata, H., Nakayama, S., Ishizuka, M., 2020a. Detoxification of lead-bearing zinc plant leach residues from Kabwe, Zambia by coupled extraction-cementation method. J. Environ. Chem. Eng. 8, 104197. https://doi.org/10.1016/j.jece.2020.104197

Silwamba, M., Ito, M., Hiroyoshi, N., Tabelin, C.B., Hashizume, R., Fukushima, T., Park, I., Jeon, S., Igarashi, T., Sato, T., Chirwa, M., Banda, K., Nyambe, I., Nakata, H., Nakayama, S., Ishizuka, M., 2020b. Recovery of Lead and Zinc from Zinc Plant Leach Residues by Concurrent Dissolution-Cementation Using Zero-Valent Aluminum in Chloride Medium. Metals 10, 531. https://doi.org/10.3390/met10040531

Smedley, P.L., Kinniburgh, D.G., 2002. A review of the source, behaviour and distribution of arsenic in natural waters. Appl. Geochem. 17, 517–568. https://doi.org/10.1016/S0883-2927(02)00018-5

Tabelin, C.B., Corpuz, R.D., Igarashi, T., Villacorte-Tabelin, M., Ito, M., Hiroyoshi, N., 2019. Hematite-catalysed scorodite formation as a novel arsenic immobilisation strategy under ambient conditions. Chemosphere 233, 946–953. https://doi.org/10.1016/j.chemosphere.2019.06.020

Tabelin, C.B., Igarashi, T., Villacorte-Tabelin, M., Park, I., Opiso, E.M., Ito, M., Hiroyoshi, N., 2018. Arsenic, selenium, boron, lead, cadmium, copper, and zinc in naturally contaminated rocks: A review of their sources, modes of enrichment, mechanisms of release, and mitigation strategies. Sci. Total Environ. 645, 1522–1553. https://doi.org/10.1016/j.scitotenv.2018.07.103

Tabelin, C.B., Park, I., Phengsaart, T., Jeon, S., Villacorte-Tabelin, M., Alonzo, D., Yoo, K., Ito, M., Hiroyoshi, N., 2021. Copper and critical metals in porphyry deposits and E-wastes: A review of resource availability, processing/recycling challenges, socio-environmental aspects, and sustainability issues. Resour. Conserv.

Recycl. accepted. https://doi.org/10.1016/j.resconrec.2021.105610

Tabelin, C.B., Sasaki, R., Igarashi, T., Park, I., Tamoto, S., Arima, T., Ito, M., Hiroyoshi, N., 2017a. Simultaneous leaching of arsenite, arsenate, selenite and selenate, and their migration in tunnel-excavated sedimentary rocks: I. Column experiments under intermittent and unsaturated flow. Chemosphere 186, 558–569. https://doi.org/10.1016/j.chemosphere.2017.07.145

Tabelin, C.B., Sasaki, R., Igarashi, T., Park, I., Tamoto, S., Arima, T., Ito, M., Hiroyoshi, N., 2017b. Simultaneous leaching of arsenite, arsenate, selenite and selenate, and their migration in tunnel-excavated sedimentary rocks: II. Kinetic and reactive transport modeling. Chemosphere 188, 444–454. https://doi.org/10.1016/j.chemosphere.2017.08.088

Tabelin, C.B., Silwamba, M., Paglinawan, F.C., Mondejar, A.J.S., Duc, H.G., Resabal, V.J., Opiso, E.M., Igarashi, T., Tomiyama, S., Ito, M., Hiroyoshi, N., Villacorte-Tabelin, M., 2020. Solid-phase partitioning and release-retention mechanisms of copper, lead, zinc and arsenic in soils impacted by artisanal and small-scale gold mining (ASGM) activities. Chemosphere 260, 127574. https://doi.org/10.1016/j.chemosphere.2020.127574

Tabelin, C.B., Veerawattananun, S., Ito, M., Hiroyoshi, N., Igarashi, T., 2017c. Pyrite oxidation in the presence of hematite and alumina: I. Batch leaching experiments and kinetic modeling calculations. Sci. Total Environ. 580, 687–698. https://doi.org/10.1016/j.scitotenv.2016.12.015

Tabelin, C.B., Veerawattananun, S., Ito, M., Hiroyoshi, N., Igarashi, T., 2017d. Pyrite oxidation in the presence of hematite and alumina: II. Effects on the cathodic and anodic half-cell reactions. Sci. Total Environ. 581–582, 126–135. https://doi.org/10.1016/j.scitotenv.2016.12.050

Tran, H.N., You, S.-J., Hosseini-Bandegharaei, A., Chao, H.-P., 2017. Mistakes and inconsistencies regarding adsorption of contaminants from aqueous solutions: A critical review. Water Res. 120, 88–116. https://doi.org/10.1016/j.watres.2017.04.014

USEPA, 2001. National Primary Drinking Water Regulations; Arsenic and Clarifications to Compliance and New Source Contaminants Monitoring. https://www.federalregister.gov/documents/2001/01/22/01-1668/national-primary-drinking-water-regulations-arsenic-and-clarifications-to-compliance-and-new-source (accessed 4.14.21)

Vithana, C.L., Sullivan, L.A., Burton, E.D., Bush, R.T., 2015. Stability of schwertmannite and jarosite in an acidic landscape: Prolonged field incubation. Geoderma 239–240, 47–57. https://doi.org/10.1016/j.geoderma.2014.09.022

WHO, 2018. Arsenic. https://www.who.int/en/news-room/fact-sheets/detail/arsenic (accessed 4.19.21)

Zhang, D., Wang, S., Wang, Y., Gomez, M.A., Jia, Y., 2019. The long-term stability of calcium arsenates: Implications for phase transformation and arsenic mobilization. J. Environ. Sci. 84, 29–41. https://doi.org/10.1016/j.jes.2019.04.017